Journal of Solid State Chemistry 181 (2008) 2713–2718

Contents lists available at ScienceDirect

Journal of Solid State Chemistry

journal homepage: www.elsevier.com/locate/jssc

Synthesis, crystal structures, and luminescent properties of two types of lanthanide phosphonates

Ya-Qin Guo [a,b], Si-Fu Tang [a], Bing-Ping Yang [a], Jiang-Gao Mao [a,*]

[a] State Key Laboratory of Structure Chemistry, Fujian Institute of Research on the Structure of Matter, Chinese Academy of Sciences, Fuzhou 350002, PR China
[b] Graduate School of the Chinese Academy of Sciences, Beijing 100039, PR China

ARTICLE INFO

Article history:
Received 25 April 2008
Received in revised form
7 June 2008
Accepted 14 June 2008
Available online 24 June 2008

Keywords:
Lanthanide phosphonates
Hydrothermal reactions
Crystal structures
Supramolecular assembly
Luminescent properties

ABSTRACT

Hydrothermal reactions of different lanthanide(III) salts with an amino-diphosphonate ligand ($H_4L = C_6H_5CH_2N(CH_2PO_3H_2)_2$) led to two series of lanthanide phosphonates, namely, $Ln(H_2L)(H_3L)$ (Ln = La, **1**; Pr, **2**; Nd, **3**; Sm, **4**; Eu, **5**; Gd, **6**; Tb, **7**). Compounds **1–5** feature a one-dimensional (1D) chain structure in which dimers of two edge-sharing LnO_8 polyhedra are interconnected by bridging phosphonate groups, such 1D arrays are further interlinked via strong hydrogen bonds between non-coordinated phosphonate oxygen atoms into a two-dimensional (2D) layer with the phenyl groups of the ligands orientated toward the interlayer space. Compounds **6** and **7** also show a different 1D array in which the LnO_6 octahedra are bridged by phosphonate groups via corner-sharing, such chains are also further interlinked by hydrogen bonds into a 2D supramolecular layer. Compounds **5** and **7** emit red and green light with a lifetime of 2.1 and 3.7 ms, respectively.

1. Introduction

Chemistry of metal phosphonates is expanding rapidly in recent years due to these compounds' versatile architectures and topologies as well as their potential applications in catalysis, ion exchange, magnetism, and materials chemistry [1–5]. The strategy of modification of the phosphonic acid with various functional groups such as crown ether, amine, hydroxyl, or/and carboxylate groups has been proven to be an extremely effective route for the construction of metal phosphonates with open framework structures [6–15]. So far, a variety of intriguing networks have been well documented in several reviews [4,16]. Lanthanide phosphonates are important since they can exhibit intense luminescence that has found applications in fluorescent probes and electroluminescent devices [17–20]. However, lanthanide phosphonates are still relatively unexplored, due to their low solubility in water and other organic solvents as well as their poor crystallinity; hence, it is still a difficult task to obtain single crystals suitable for X-ray structural analysis. Results from our previous studies indicate that phosphonic acid, in conjunction with a suitable ancillary ligand such as 5-sulfoisophthalic acid (H_3BTS) or oxalate, is an effective route for the preparation of crystalline lanthanide phosphonates [21–23]. Another useful alternative method is the use of the phosphonic acid attached with functional groups with additional coordination atoms such as the carboxylate acid or amino acid [24–27]. As an extension of our previous work, in this work we used an amino-diphosphonate ligand, *N*-benzyliminobis(methylenephosphonic acid), $C_6H_5CH_2N(CH_2PO_3H_2)_2$ (H_4L), whose transition metal complexes have been reported to exhibit two-dimensional (2D) layers or one-dimensional (1D) arrays [28–31]. We hope to get better understandings of the effects of different metal cations on the final structures and the photoluminescence properties. Our research efforts afforded two series of lanthanide phosphonates, namely, $Ln(H_2L)(H_3L)$ (Ln = La, **1**; Pr, **2**; Nd, **3**; Sm, **4**; Eu, **5**) and $Ln(H_2L)(H_3L)$ (Ln = Gd, **6**; Tb, **7**). Both types of compounds feature 2D supramolecular networks based on 1D arrays interconnected via hydrogen bonds.

2. Experimental section

2.1. Materials and methods

$LnCl_3 \cdot nH_2O$ (Ln = La, Pr, Nd, Sm, Eu, Gd, Tb) were prepared by dissolving lanthanide oxide in hydrochloric acid, and then the mixture was heated at ~100 °C in the air until a lot of powder appeared. $C_6H_5CH_2N(CH_2PO_3H_2)_2$ (H_4L) were prepared by a Mannich-type reaction according to procedures described previously [32–34]. All other chemicals were obtained from commercial sources and used without further purification. Elemental analyses (C, H, and N) were carried out on a Vario EL III elemental analyser. IR spectra were recorded on a Magna 750 FT-IR

* Corresponding author. Fax: +86 591 83714946.
E-mail address: mjg@fjirsm.ac.cn (J.-G. Mao).

0022-4596/$ - see front matter © 2008 Elsevier Inc. All rights reserved.
doi:10.1016/j.jssc.2008.06.043

spectrophotometer using KBr pellets in the range 4000–400 cm^{-1}. Thermal gravimetric analyses (TGA) analysis was performed on a NETZSCH STA 449C unit under oxygen flow at a heating rate of 10 °C min^{-1}. Photoluminescence analyses were performed on a Perkin-Elemer LS55 fluorescence spectrometer. XRD powder patterns (Cu$K\alpha$) were collected on an XPERT-MPD 2θ diffractometer.

2.2. Syntheses of $Ln(H_2L)(H_3L)$ (Ln = La, 1; Pr, 2; Nd, 3; Sm, 4; Eu, 5)

A mixture of $LnCl_3 \cdot nH_2O$ (0.25 mmol), H_4L (0.295 g, 1 mmol) in 10 mL of distilled water was sealed in an autoclave equipped with a Teflon liner (23 mL) and its pH value is ~1. Then the solution was heated at 165 °C for 5 days. Crystals of **1** (colourless), **2** (green), **3** (purple), **4** (colourless), and **5** (yellow) were collected in ca. yields of 78%, 81%, 82%, 73%, and 75% (based on lanthanide), respectively. The measured XRD patterns are comparable with the simulated ones (see Supporting Information). Anal. Calcd. for $C_{18}H_{27}N_2O_{12}P_4La$: C, 29.77; H, 3.75; N, 3.86%. Found: C, 29.49; H, 3.98; N, 3.68%. IR data (KBr, cm^{-1}): 3005 (m), 2944 (m), 2815 (m), 2746 (m), 2601 (m), 1458 (m), 1249 (s), 1170 (s), 1118 (s), 920 (m), 852 (w), 811 (w), 738 (m), 588 (m), 565 (w), 531 (m). Anal. Calcd. for $C_{18}H_{27}N_2O_{12}P_4Pr$: C, 29.69; H, 3.74; N, 3.85%. Found: C, 29.48; H, 3.96; N, 3.61%. IR data (KBr, cm^{-1}): 3007 (m), 2945 (m), 2813 (m), 2745 (m), 2565 (m), 1458 (m), 1249 (s), 1171 (s), 1134 (s), 920 (m), 740 (m), 589 (w), 567 (w), 531 (m). Anal. Calcd. $C_{18}H_{27}N_2O_{12}P_4Nd$: C, 29.55; H, 3.72; N, 3.83%. Found: C, 29.32; H, 3.89; N, 3.63%. IR data (KBr, cm^{-1}): 3007 (m), 2944 (m), 2814 (m), 2745 (m), 2595 (m), 1458 (m), 1248 (s), 1171 (s), 1134 (s), 920 (m), 895 (m), 739 (m), 589 (w), 569 (w), 530 (m). Anal. Calcd. for $C_{18}H_{27}N_2O_{12}P_4Sm$: C, 29.31; H, 3.69; N, 3.80%. Found: C, 29.02; H, 3.91; N, 3.65%. IR data (KBr, cm^{-1}): 3008 (m), 2956 (m), 2813 (m), 2746 (m), 2546 (m), 1459 (m), 1249 (s), 1173 (s), 1133 (s), 920 (m), 740 (m), 590 (w), 568 (w), 530 (m). Anal. Calcd. for $C_{18}H_{27}N_2O_{12}P_4Eu$: C, 29.24; H, 3.68; N, 3.79%. Found: H, 3.95; C, 28.06; N, 3.57%. IR data (KBr, cm^{-1}): 3007 (m), 2946 (m), 2814 (m), 2746 (m), 2545 (m), 1458 (m), 1248 (s), 1172 (s), 1134 (s), 920 (m), 739 (m), 589 (w), 569 (w), 530 (m).

2.3. Syntheses of $Ln(H_2L)(H_3L)$ (Ln = Gd, 6; Tb, 7)

A mixture of $LnCl_3 \cdot 6H_2O$ (0.25 mmol), H_4L (0.295 g, 1 mmol) in distilled water (10 mL) was sealed in an autoclave equipped with a Teflon liner (23 mL) and its pH value is ~1. Then the solution was heated at 165 °C for 5 days. Needle-like crystals of **6** (colourless) and **7** (colourless) were collected in ca. 64% and 82% yield (based on lanthanide), respectively. The measured XRD powder patterns are comparable with the simulated ones (see Supporting Information). Anal. Calcd. for $C_{13}H_{27}N_2O_{12}P_4Gd$: C, 29.04; H, 3.66; N, 3.76%. Found: C, 28.78; H, 3.82; N, 3.57%. IR data (KBr, cm^{-1}): 3007 (m), 2945 (m), 2850 (m), 2745 (m), 2545 (m), 1458 (m), 1247 (s), 1172 (s), 1133 (s), 920 (m), 739 (m), 589 (w), 568 (w), 529 (m). Anal. Calcd. for $C_{13}H_{27}N_2O_{12}P_4Tb$: C, 28.97; H, 3.65; N, 3.75%. Found: C, 28.65; H, 3.78; N, 3.56%. IR data (KBr, cm^{-1}): 3007 (m), 2966 (m), 2756 (m), 2722 (m), 1430 (m), 1246 (s), 1164 (s), 1099 (s), 912 (m), 739 (m), 591 (m), 565 (m), 535 (m).

2.4. Single-crystal structure determination

Based on the measured XRD powder patterns, compounds **1–5** are isostructural, so are compounds **6** and **7** (see Supporting Information). Therefore, only compounds **4** and **7** were subject to single-crystal structural analyses. Date collections for compounds **4** and **7** were performed on a Siemens Smart CCD diffractometer equipped with graphite-monochromated Mo$K\alpha$ radiation ($\lambda = 0.71073$ Å). Intensity data were collected by the narrow frame method at 293 K and corrected for Lorentz and polarization effects as well as for absorption by the SADABS programme [35,36]. Both structures were solved by direct methods and refined by full-matrix least-squares cycles in SHELX-97 [37]. All non-hydrogen atoms were refined with anisotropic thermal parameters. Hydrogen atoms attached to the C and N atoms were located at geometrically calculated positions and refined with isotropic thermal parameters. Crystallographic data and structural refinement parameters for compounds **4** and **7** are summarized in Table 1. Important bond distances are listed in Table 2.

CCDC-684385 (**4**) and CCDC-684386 (**7**) contain the supplementary crystallographic materials for this paper. These data can be obtained free of charge from The Cambridge Crystallographic Data Center via www.ccdc.cam.ac.uk/data_request/cif.

3. Results and discussion

The isolations of compounds **1–7** rely on the hydrothermal techniques. Results indicate that the reaction conditions play an important role in the formation of the title compounds. Pure phases were obtained at the L/Ln ratio of 4:1, low pH values of the reaction mixture favour the protonation of some phosphonate groups and facilitate the formation of low-dimensional coordination polymers. When the L/Ln ratio is less than 1:1 at the same conditions, we could not obtain the single crystals but only unknown precipitates.

3.1. Structure description for $Ln(H_2L)(H_3L)$ (Ln = La, 1; Pr, 2; Nd, 3; Sm, 4; Eu, 5)

Compounds **1–5** are isostructural, hence the structure of compound **4** was described representatively. The asymmetric unit of **4** consists of a Sm(III) ion, a $\{H_2L\}^{2-}$ and a $\{H_3L\}^{-}$ anion (Fig. 1). The Sm(III) center is eight-coordinated by three oxygen atoms from three $\{H_3L\}^{-}$ anions and five oxygen atoms from three $\{H_2L\}^{2-}$ anions. The Sm–O distances are in the range of 2.345(5)–2.725(6) Å. The two phosphonate ligands adopt two different types of coordination modes (Scheme 1). The $\{H_3L\}^{-}$ anion acts as a tridentate ligand, one phosphonate group is monodnetate whereas the other one is bidentate bridging (Scheme 1a), both phosphonate groups are singly protonated (O7, O11) based on P–O distances (Table 2), so is the amine group.

Table 1
Crystal data and structure refinements for **4** and **7**

Compound	**4**	**7**
Formula	$C_{18}H_{27}N_2O_{12}P_4Sm$	$C_{18}H_{27}N_2O_{12}P_4Tb$
fw	737.65	746.22
Crystal system	Triclinic	Orthorhombic
Space group	$P\bar{1}$	$P2_12_12_1$
a (Å)	8.056(3)	7.994(2)
b (Å)	12.755(5)	25.351(7)
c (Å)	13.498(7)	25.589(8)
α (deg)	115.395(9)	90
β (deg)	92.49(2)	90
γ (deg)	93.030(2)	90
V (Å^3)	1247.8(9)	5186(3)
Z	2	8
D_c (g cm^{-3})	1.963	1.911
μ (mm^{-1})	2.676	3.038
R_1, wR_2 [$I > 2\sigma(I)$]	$R1 = 0.0545$, w$R2 = 0.1441$	$R1 = 0.0587$, w$R2 = 0.1133$
R_1, wR_2 (all data)	$R1 = 0.0576$, w$R2 = 0.1460$	$R1 = 0.0780$, w$R2 = 0.1267$
GOF[c]	1.087	1.093

$R_1 = \Sigma\|\|F_0\|-\|F_c\|\|/\Sigma|F_0|$, w$R_2 = \Sigma[w(F_0^2-F_c^2)^2]/\Sigma[w(F_0^2)^2]^{1/2}$.

Table 2
Selected bond lengths (Å) for **4** and **7**

Compound **4**			
Sm(1)–O(8)	2.345(5)	Sm(1)–O(6)♯1	2.360(5)
Sm(1)–O(9)♯2	2.380(5)	Sm(1)–O(10)♯3	2.390(5)
Sm(1)–O(1)	2.428(5)	Sm(1)–O(3)♯3	2.542(6)
Sm(1)–O(2)♯3	2.550(5)	Sm(1)–O(3)	2.725(6)
P(1)–O(1)	1.504(5)	P(1)–O(2)	1.525(5)
P(1)–O(3)	1.533(6)	P(2)–O(4)	1.507(6)
P(2)–O(6)	1.493(5)	P(2)–O(5)	1.581(5)
P(3)–O(8)	1.497(5)	P(3)–O(7)	1.584(5)
P(3)–O(9)	1.489(5)	P(4)–O(10)	1.485(6)
P(4)–O(11)	1.579(5)	P(4)–O(12)	1.504(5)
Compound **7**			
Tb(1)–O(7)	2.211(6)	Tb(1)–O(15)♯1	2.241(6)
Tb(1)–O(3)♯1	2.247(7)	Tb(1)–O(5)	2.279(6)
Tb(1)–O(20)	2.292(6)	Tb(1)–O(24)♯1	2.297(6)
Tb(2)–O(1)	2.223(6)	Tb(2)–O(19)	2.237(6)
Tb(2)–O(8)	2.279(6)	Tb(2)–O(11)♯2	2.279(6)
Tb(2)–O(14)	2.282(7)	Tb(2)–O(18)♯1	2.295(6)
P(1)–O(2)	1.512(7)	P(1)–O(3)	1.522(7)
P(1)–O(1)	1.528(6)	P(2)–O(4)	1.488(7)
P(2)–O(5)	1.502(6)	P(2)–O(6)	1.568(7)
P(3)–O(7)	1.493(7)	P(3)–O(8)	1.503(7)
P(3)–O(9)	1.537(7)	P(4)–O(10)	1.498(7)
P(4)–O(11)	1.505(7)	P(4)–O(12)	1.557(7)
P(5)–O(14)	1.497(7)	P(5)–O(15)	1.519(6)
P(5)–O(13)	1.530(7)	P(6)–O(16)	1.495(7)
P(6)–O(18)	1.499(7)	P(6)–O(17)	1.565(7)
P(7)–O(20)	1.499(6)	P(7)–O(19)	1.503(7)
P(7)–O(21)	1.544(7)	P(8)–O(22)	1.573(7)
P(8)–O(24)	1.490(7)	P(8)–O(23)	1.493(7)

Symmetry transformations used to generate equivalent atoms:
For 4: ♯1 $x-1, y, z$; ♯2 $-x-1, -y, -z+1$; ♯3 $-x, -y, -z+1$.
For 7: ♯1 $x-1, y, z$; ♯2 $x+1, y, z$.

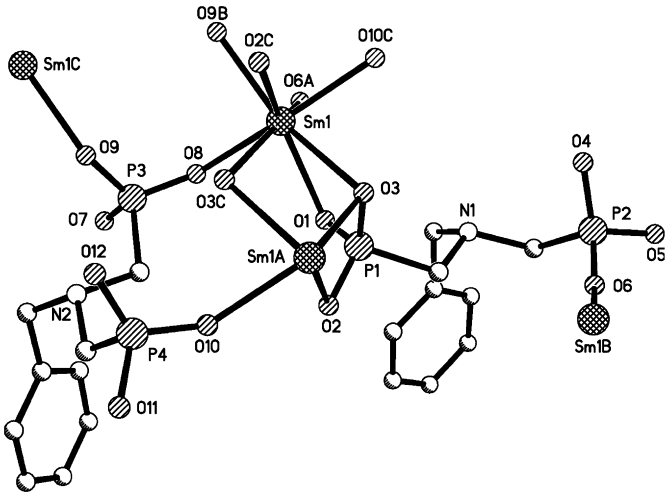

Fig. 1. ORTEP drawing of compound **4** with atom-labeling scheme. Hydrogen atoms are omitted for clarity. Symmetry codes for the generated atoms: (a) $x-1, y, z$; (b) $-x-1, -y, -z+1$; (c) $-x, -y, -z+1$.

Such coordination mode is also reported in $M\{H_3L\}_2$ (M = Mn, Cd) [28,31]. The $\{H_2L\}^{2-}$ anion functions as a tetradentate ligand, being chelating bidentately to two metal centres by using one phosphonate group and also bridges to the third Sm(III) atom (Scheme 1b) via the other phosphonate group, one phosphonate oxygen atom (O5) is singly protonated based on P–O distance, so is the amine group.

Each pair of Sm(III) ions is bridged by a pair of phosphonate groups (Sm–O–Sm and Sm–O–P–O–Sm bridges) of two $\{H_2L\}^{2-}$ anions into a dimeric unit with a Sm⋯Sm separation of 4.390(1) Å, neighbouring dimers are further interconnected by a

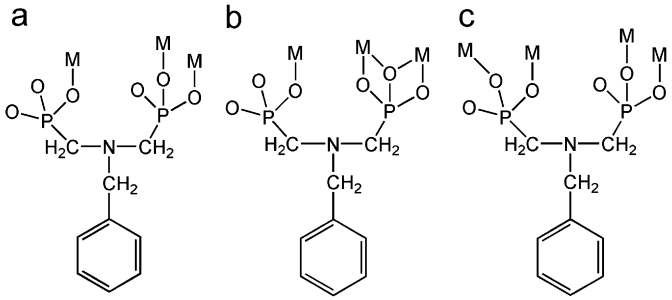

Scheme 1. Coordination fashions of phosphonate ligands in compounds **4** and **7** as well as its transition metal complexes.

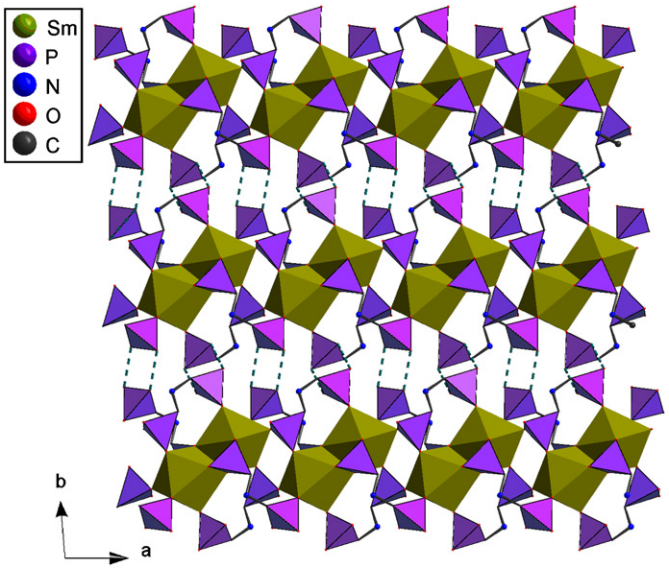

Fig. 2. A 2D supramolecular layer based on 1D chains of lanthanide(III) phosphonates in **4**. Hydrogen bonds are represented by the dashed lines.

pair of phosphonate groups from two $\{H_3L\}^-$ anions into a 1D chain along the *a*-axis (Fig. 2). Within the chain, intra-chain hydrogen bonds are formed between protonated amine groups and non-coordination phosphonate oxygen atoms. The corresponding hydrogen bond lengths and angles are 2.635(8) and 2.756(8) Å, 156.2° and 154.1°, respectively (Table 3). Adjacent samarium(III) phosphonate chains are further interlinked via hydrogen bonds between the non-coordinated phosphonate oxygen atoms into a 2D sheet (Fig. 2). The hydrogen bond distances range from 2.579(7) to 2.648(8) Å and bond angles from 160.69° to 172.64°, respectively (Table 3). The phenyl rings of the ligands are hanging on the interlayer space. These 2D sheets are further held together via $\pi-\pi$ stacking interactions between the phenyl groups into a three-dimensional (3D) supramolecular framework (Fig. 3). The close contact distance between adjacent aromatic rings is ca. 3.45 Å.

3.2. *Structure description for $Ln(H_2L)(H_3L)$ (Ln = Gd, 6; Tb, 7)*

Compounds **6** and **7** feature a different 1D lanthanide(III) phosphonate chain from that of **1–5**. As illustrated in Fig. 4, the asymmetric unit of **7** contains two crystallographically independent Tb(III) atoms, two $\{H_2L\}^{2-}$ and two $\{H_3L\}^-$ anions (Fig. 4). Unlike the lanthanide(III) ions in **1–5**, both Tb(III) ions in **7** are octahedrally coordinated by six oxygen atoms from three $\{H_2L\}^{2-}$ and three $\{H_3L\}^-$ anions. The smaller coordination numbers for

Table 3
Hydrogen bonding geometry (distances in Å and angles in °)

D–H···A	d(D–H)	d(H···A)	<DHA	d(D···A)
Compound ***4***				
N1–H1A···O12^{i}	0.910	1.777	156.17	2.635(8)
N2–H2A···O4^{i}	0.910	1.908	154.11	2.756(8)
O5–H5A···O4^{ii}	0.820	1.787	167.34	2.593(8)
O7–H7C···O2^{iii}	0.820	1.790	160.69	2.579(7)
O11–H11A···O12^{iv}	0.820	1.832	172.64	2.648(8)
Compound ***7***				
N1–H1A···O23	0.910	1.929	150.97	2.76(1)
N2–H2A···O16^{iii}	0.910	1.883	152.68	2.72(1)
N3–H3A···O10^{v}	0.910	1.957	147.91	2.77(1)
N4–H4A···O4	0.910	1.893	152.85	2.73(1)
O6–H6A···O10^{vi}	0.820	1.785	172.07	2.599(9)
O9–H9C···O2^{iii}	0.820	1.699	172.78	2.51(1)
O12–H12A···O4^{vii}	0.820	1.846	168.70	2.66(1)
O17–H17C···O23^{viii}	0.820	1.821	172.52	2.636(9)
O21–H21A···O13	0.820	1.698	168.79	2.507(9)
O22–H22A···O16^{ix}	0.820	1.874	168.90	2.68(1)

Symmetry transformations used to generate equivalent atoms:
(i) $-x, -y, -z+1$; (ii) $-x+1, -y-1, -z+1$; (iii) $x-1, y, z$; (iv) $-x, -y+1, -z+1$; (v) $x+1, y, z$; (vi) $-x, y-1/2, -z+1/2$; (vii) $-x, y+1/2, -z+1/2$; (viii) $-x+2, y+1/2, -z+1/2$; (ix) $-x+2, y-1/2, -z+1/2$.

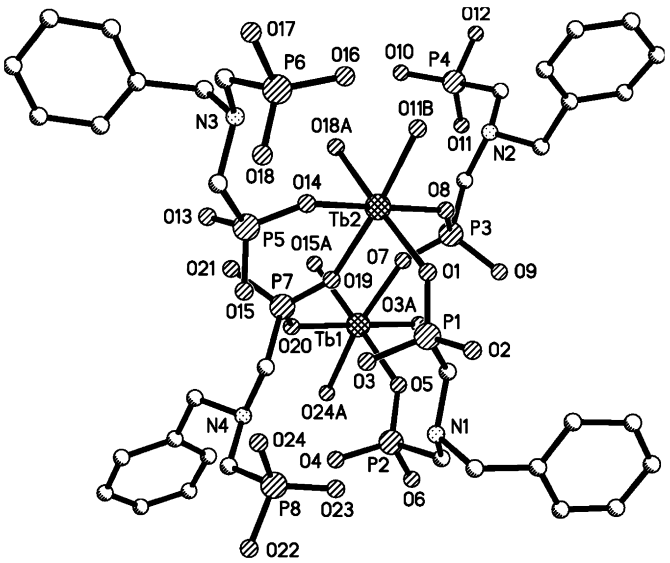

Fig. 4. ORTEP view of the asymmetric unit of compound **7**. Hydrogen atoms as well as the phenyl rings of the phosphonate ligands were omitted for clarity. Symmetry codes for the generated atoms: (a) $x-1, y, z$; (b) $x+1, y, z$.

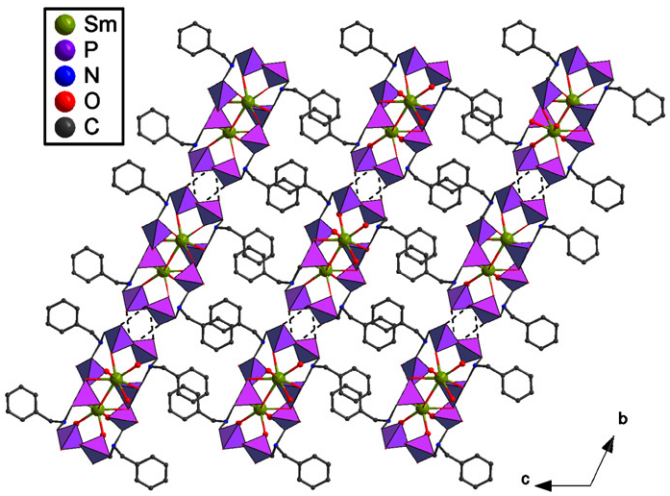

Fig. 3. View of the structure of **4** down the *a*-axis. Hydrogen bonds are represented by the dashed lines.

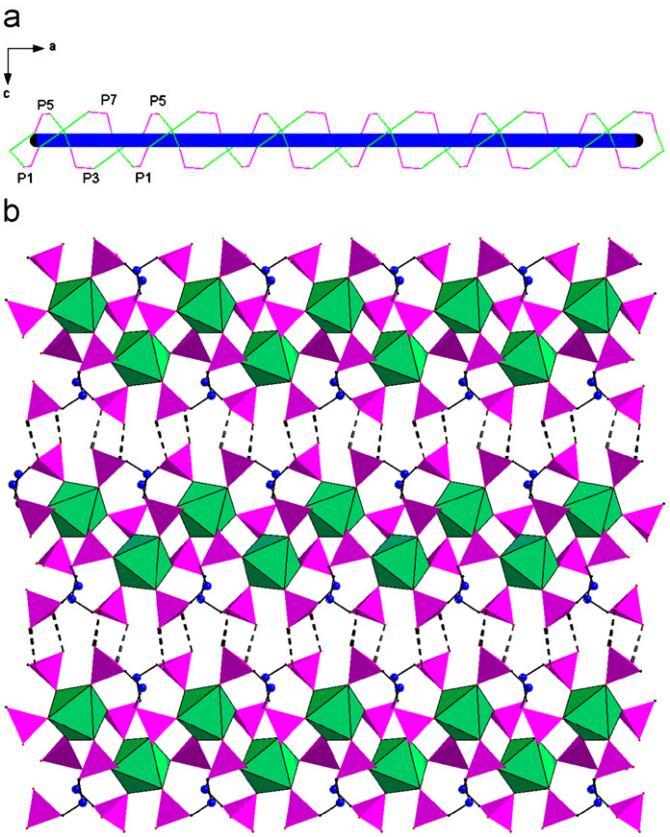

Fig. 5. (a) Wire representation of a racemic terbium phosphonate chain, (b) a 2D supramolecular layer based on 1D chains of lanthanide(III) phosphonates in **7**. CPO_3 tetrahedra are in purple; Tb octahedra, green; N, C and O atoms are drawn as blue, grey and red, respectively. Hydrogen bonds are represented by the dashed lines.

Gd(III) and Tb(III) ions compared to those for La–Eu is due to the so-called "lanthanide contraction". The Tb–O bond lengths fall in the range 2.211(6)–2.297(6) Å (Table 2), which are slightly shorter than Sm–O bonds in **4**. Both $\{H_2L\}^{2-}$ and $\{H_3L\}^{-}$ anions are tridentate and bridge with three Tb(III) ions (Scheme 1a), one $\{CPO_3\}$ group is monodentate, whereas the other one is bidentate. Such coordination mode has also been observed in **4**. The amine groups of both $\{H_2L\}^{2-}$ and $\{H_3L\}^{-}$ anions are protonated, but the protonation of phosphonate groups are different: both phosphonate groups are singly protonated in the $\{H_3L\}^{-}$ anion whereas only one phosphonate group is singly protonated in the $\{H_2L\}^{2-}$ anion.

The Tb^{3+} ions are bridge by the $\{CPO_3\}$ groups to form an infinite chain running along the *a*-axis (Fig. 5a). Such chain is racemic since it is composed of right-handed helical chain formed by Tb(1) bridged by P(3)O_3 and P(5)O_3 groups, and left-handed helical chain formed by Tb(1) bridged by P(1)O_3 and P(7)O_3 groups. Intra-chain hydrogen bonds are formed between amine groups and non-coordination phosphonate oxygen atoms, the N–H···O bond lengths range from 2.72(1) to 2.77(1) Å (Table 3). These chains are further interconnected via extensive interchain hydrogen bonds, resulting in a 2D supramolecular assembly (Fig. 5b). The O–H···O bond lengths are in the range of

2.507(9)–2.683(10) Å and the corresponding bond angles are in the range of 168.70–172.78° (Table 3). Unlike those in compound **4**, the phenyl rings are not parallel to each other, hence there are no π–π stacking interactions and these 2D layers are held together via van der Waals interactions (Fig. 6). The structure of **7** is in fact identical to those of the transition metal complexes, $M\{H_3L\}_2$ (M = Mn, Cd) [28,31], the only difference lie in that the higher positive charge of Tb^{3+} ion compared to M^{2+} forces one more proton to be removed from a $\{H_3L\}^-$ anion to become a $\{H_2L\}^{2-}$ anion which lowers the symmetry of metal ion from C_i to C_1. The 1D chain of compound **7** is different from that of 4 in that it lacks the Ln–O–Ln bridges and Tb^{3+} ion has a lower coordination number, which is due to the different coordination modes adopted for the $\{H_2L\}^{2-}$ anions as well as the so-called lanthanide contraction. It should be also mentioned that under higher pH value, $Mn(H_2L)$ with a layered structure is formed in which the phosphonate anion adopts a different coordination mode: tetradentate and bridging with four metal centres (Scheme 1c) [31].

3.3. TGA and luminescence properties studies for compounds 4 and 7

TGA were conducted to examine the stabilities of these compounds. Compounds **1–7** show similar TGA curves and compounds **4** and **7** were used as two representatives (Fig. 7, see also Supporting Materials). The TGA curves of **4** displays two major steps of weight losses. The first weight loss of 30.2% between 310 and 552 °C can be attributed to the release of water molecules formed by condensation of two protonated phosphonate groups and combustion of organic groups. The second step in the temperature of 800–1000 °C corresponds to further decomposition of the phosphonate ligands. The total weight loss at 1052 °C is 58.9% and the residuals were not characterized due to its corrosion with the container (Al_2O_3 crucible). TGA curves of compound **7** also show two major weight losses. The first weight loss of 28.6% in the temperature of 294–575 °C corresponds to the release of water molecules formed by condensation of two protonated phosphonate groups and combustion of organic groups. The second weight loss of 32.7% from 860 to 1060 °C is due to the further decomposition of the organic groups. The total weight loss at 1060 °C is 61.3% and the residuals were not identified due to their reactions with the container (Al_2O_3 crucible).

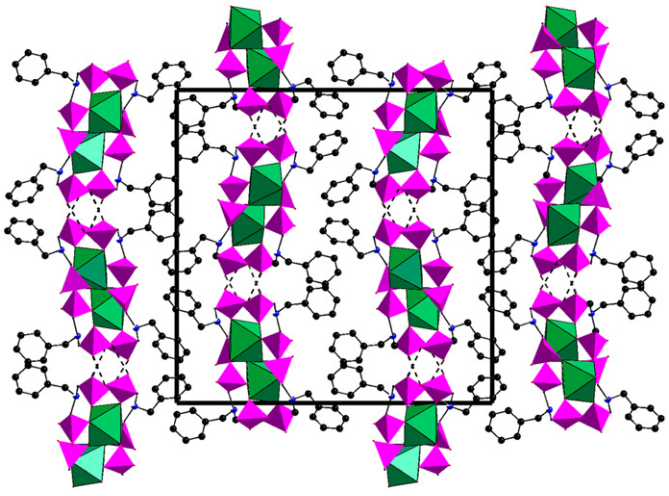

Fig. 6. View of the structure of **7** down the a-axis. CPO_3 tetrahedra are in purple; Tb octahedra, green; N, C and O atoms are drawn as blue, black and red, respectively. Hydrogen bonds are represented by the dashed lines.

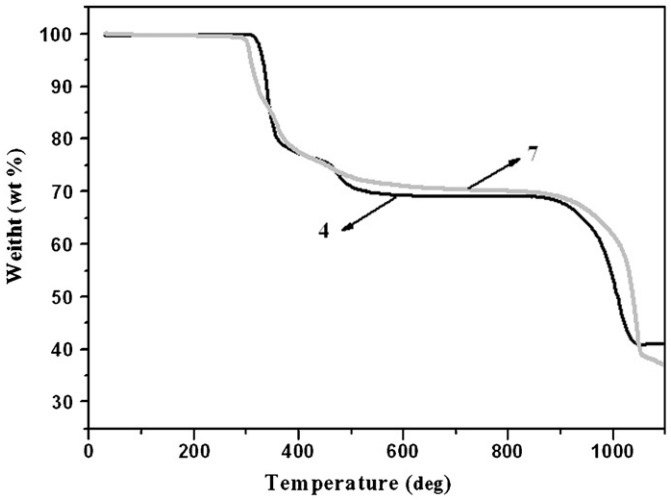

Fig. 7. TGA curves for compounds **4** and **7**.

The solid-state luminescent properties of compounds **5** and **7** are measured at room temperature (Fig. 8). The free H_4L exhibits a broad fluorescent emission band at 417 nm under excitation at 370 nm, which can be assigned to the intra-ligand π–π^* transition (see Supporting Materials). Upon complexion with lanthanide(III) ion, only sharp emission bands associated with corresponding lanthanide(III) ions were observed, indicating the complete energy transfer from the phosphonate ligands to the central lanthanide ions [21,22,24,26]. Upon excitation at 394 nm, compound **5** displays characteristic emission bands in the 570–720 nm region, corresponding to the $^5D_o \rightarrow {}^7F_n$ (n = 0–4) transitions of Eu^{3+} ion (Fig. 8a). The $^5D_0 \rightarrow {}^7F_2$ transition, which is electric dipole allowed and hypersensitive to chemical bonds in the vicinity of Eu (III) ion, is very intense, emitting strong red luminescence. The presence of only one sharp band for the $^5D_0 \rightarrow {}^7F_0$ transition confirms the existence of only one type of Eu(III) cation with a C1 symmetry. The Eu ($^5D_0$) lifetime of compound **5** for $\lambda_{ex,em}$ = 394 and 616 nm is measured to be about 2.1 ms.

The luminescent spectrum of **7** (Fig. 8b) excited at 268 nm exhibits the emissions bands associated with $^5D_4 \rightarrow {}^7F_j$ (j = 3,4,5,6) of the Tb^{3+} ion. All of transition bands split into two sub-bands, which is due to crystal field splitting as well as the presence of two unique Tb(III) sites in the structure. The most-intense emission appears at 550 nm in the green light region. The Tb ($^5D_4$) lifetime of compound **7** for $\lambda_{ex,em}$ = 368 and 616 nm is 3.7 ms.

The non-centrosymmetric structures of compounds **6** and **7** (space group $P2_12_12_1$) prompt us to measure their SHG properties. Unfortunately, SHG measurements on the powder samples indicated that their SHG signals are not observed, this is reasonable since the 1D lanthanide phosphonate chains are racemic.

4. Conclusion

The systematic investigations of the reactions between *N*-benzyliminobis(methylenephosphonic acid) and lanthanide salts resulted in two types of 1D coordination polymers. The structures of complexes **1–7** are completely different despite of their similar structural formulae. Compounds **1–5** feature a chain structure in which dimers of edge-sharing LnO_8 polyhedra are further interconnected by phosphonate ligands. For compounds **6** and **7**, the 1D chain structure is formed by Ln(III) ions interconnected via Ln–O–P–O–Ln bridges. The differences between the two types of compounds stem from different

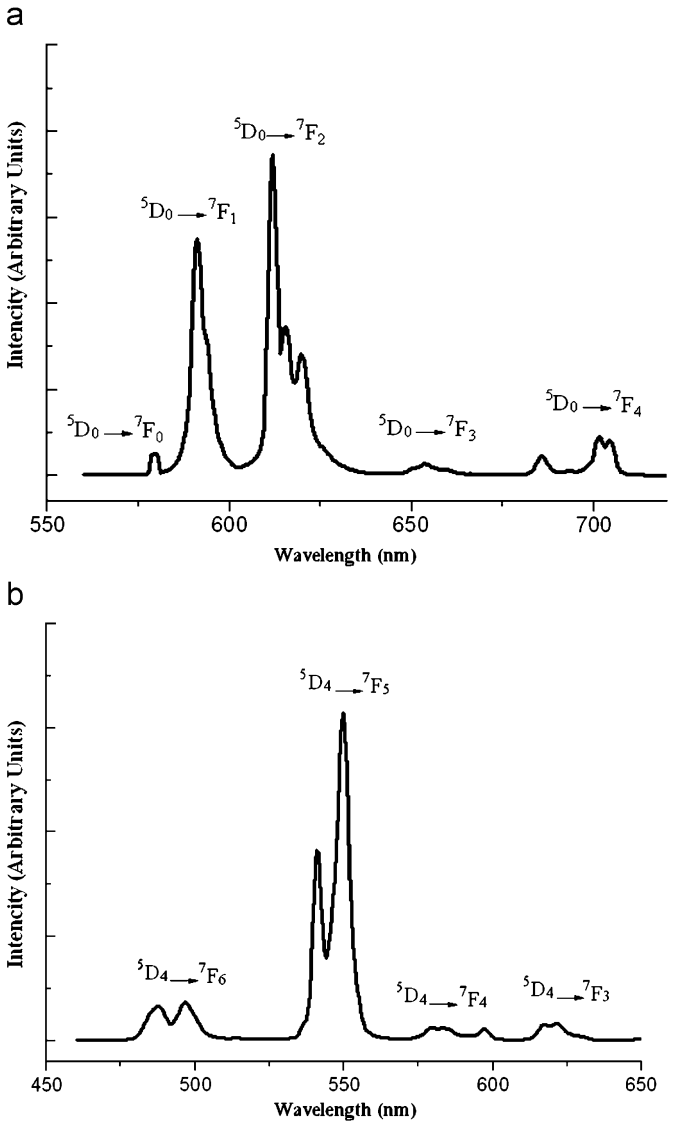

Fig. 8. Solid-state emission spectra of compounds **5** (a) and **7** (b).

coordination modes of the phosphonate ligand as well as the effect of lanthanide contraction. Strong intra- and inter-chain hydrogen bonds are formed in both types of compounds. Future research efforts will be devoted to the study of the effect of the second ligand such as bipy or phen on the structures of lanthanide phosphonates.

Acknowledgments

This work was financially supported by National Natural Science Foundation of China (nos. 20371047 and 20521101), the NSF of Fujian Province (no. E0610034), Key Project of Chinese Academy of Sciences (no. KJCX2-YW-H01) and 973 Programme (no. 2006CB932903).

Appendix A. Supplementary materials

Supplementary materials associated with this article can be found in the online version at doi:10.1016/j.jssc.2008.06.043.

References

[1] A. Clearfield, Prog. Inorg. Chem. 37 (1998) 371–510.
[2] K. Maeda, Micro. Meso. Mater. 73 (2004) 47–55 and references therein.
[3] A. Inoue, H. Shinokubo, K. Oshima, J. Am. Chem. Soc. 125 (2003) 1484–1485.
[4] E. Matczak-Jon, V. Videnova-Adrabińska, Coord. Chem. Rev. 249 (2005) 2458–2488.
[5] M. Shanmugam, G. Chastanet, T. Mallah, R. Sessoli, S.J. Teat, G.A. Timco, R.E.P. Winpenny, Chem. Eur. J. 12 (2006) 8777–8785.
[6] J.A. Groves, N.F. Stephens, P.A. Wright, W.P. Lightfoot, Solid State Sci. (2006) 397–403.
[7] Y. Qi, J. Yang, G.-H. Li, G.-D. Li, J.-S. Chen, Inorg. Chem. 45 (2006) 4431–4439.
[8] X.-M. Zhang, J.-J. Hou, W.-X. Zhang, X.-M. Chen, Inorg. Chem. 45 (2006) 8120–8125.
[9] J.A. Groves, P.A. Wright, W.P. Lightfoot, Inorg. Chem. 44 (2005) 1736–1739.
[10] J.A. Groves, S.R. Miller, S.J. Warrender, C. Mellot-Draznieks, P. Lighfoot, P.A. Wright, Chem. Commun. (2006) 3305–3307.
[11] C.V.K. Sharma, A. Clearfield, J. Am. Chem. Soc. 122 (2000) 1558–1559.
[12] S. Bauer, N. Stock, Angew. Chem. Int. Ed. 46 (2007) 6857–6860.
[13] N. Stock, T. Bein, Angew. Chem. Int. Ed. 43 (2004) 749–752.
[14] R. Murugavel, S. Kuppuswamy, R. Boomishankar, A. Steiner, Angew. Chem. Int. Ed. 45 (2006) 5536–5540.
[15] D.-K. Cao, J. Xiao, J.-W. Tong, Y.-Z. Li, L.-M. Zheng, Inorg. Chem. 46 (2007) 428–436.
[16] J.-G. Mao, Coord. Chem. Rev. 251 (2007) 1493–1520.
[17] J.M. Lehn, Angew. Chem. Int. Ed. English 29 (1990) 1304–1319.
[18] B. Zhao, X.-Y. Chen, P. Cheng, D.-Z. Liao, S.-P. Yan, Z.-H. Jiang, J. Am. Chem. Soc. 126 (2004) 15394–15395.
[19] S.-S. Bao, L.-F. Ma, Y. Wang, L. Fang, C.-J. Zhu, Y.-Z. Li, L.-M. Zheng, Chem. Eur. J. 13 (2007) 2333–2343.
[20] Y.-J. Kim, M.-K. Suh, D.-Y. Jung, Inorg. Chem. 43 (2004) 245–250.
[21] J.L. Song, J.G. Mao, Chem. Eur. J. 11 (2005) 1417–1424.
[22] S.-M. Ying, J.-G. Mao, Cryst. Growth Des. 6 (2006) 964–968.
[23] J.L. Song, C. Lei, J.G. Mao, Inorg. Chem. 43 (2004) 5630–5634.
[24] S.-F. Tang, J.-L. Song, X.-L. Li, J.-G. Mao, Cryst. Growth Des. 6 (2007) 360–366.
[25] S.-F. Tang, J.-L. Song, J.-G. Mao, Eur. J. Inorg. Chem. (2006) 2011–2019.
[26] S.-F. Tang, J.-L. Song, X.-L. Li, J.-G. Mao, Cryst. Growth Des. 6 (2006) 2322–2326.
[27] C. Serre, N. Stock, T. Bein, G. Férey, Inorg. Chem. 43 (2004) 3159–3163.
[28] Z.-M. Sun, B.-P. Yang, Y.-Q. Sun, J.-G. Mao, A. Clearfield, J. Solid State Chem. 176 (2003) 62–68.
[29] Z.-M. Sun, J.-G. Mao, Y.-Q. Sun, H.-Y. Zeng, A. Clearfield, New J. Chem. 27 (2003) 1326–1330.
[30] Z.-M. Sun, J.-G. Mao, B.-P. Yang, S.-M. Ying, Solid State Sci. 6 (2004) 295–300.
[31] Z.-M. Sun, J.-G. Mao, Z.-C. Dong, Polyhedron 24 (2005) 571–577.
[32] J.-G. Mao, Z.-K. Wang, A. Clearfield, Inorg. Chem. 41 (2002) 2334–2340.
[33] J.-G. Mao, Z.-K. Wang, A. Clearfield, Inorg. Chem. 41 (2002) 6106–6111.
[34] J.-G. Mao, Z.-K. Wang, A. Clearfield, J. Chem. Soc. Dalton Trans. (2002) 4457–4463.
[35] G.M. Sheldrick, Program SADABS, Universität Göttingen, 1995.
[36] CrystalClear ver. 1.3.5. Rigaku Corporation, Woodlands, TX, 1999.
[37] G.M. Sheldrick, SHELXTL, Crystallographic Software Package, SHELXTL, Version 5.1, Bruker-AXS, Madison, WI, 1998.